

*Original Article*

## Assessment of ultimate load of built-up slot-in cold-formed steel column filled with polyurethane foam

Mohd Syahrul Hisyam Mohd Sani<sup>1\*</sup>, Mohd Risham Jaafar<sup>1</sup>, Bishir Kado<sup>2</sup>, Ahmad Rasidi Osman<sup>1</sup>, and Fadhluhartini Muftah<sup>1</sup>

<sup>1</sup> Faculty of Civil Engineering, Universiti Teknologi MARA (UiTM) Pahang Branch, Bandar Jengka, Pahang, 26400 Malaysia

<sup>2</sup> Department of Civil Engineering, Faculty of Engineering, Bayero University, Kano, Nigeria

Received: 23 August 2024; Revised: 6 February 2025; Accepted: 8 April 2025

---

### Abstract

Cold-formed steel (CFS) is a steel-based material that has always been used in construction activity and has shown a lot of advantages. However, CFS is exposed to buckling failure under axial compression load due to a thin surface or slender section. There are many methods to solve the buckling failure in the initial stage such as the production of a built-up CFS section and the production of a built-up CFS section with other materials to form a composite section. Thus, the built-up slot-in CFS column is established by using self-drilling screws and filled with polyurethane foam (PF), for which no information about such composite column is available in prior studies. The main objective of the study is to assess the ultimate load of the built-up slot-in CFS column filled with PF and observe the failure mode of all specimens. In this research design, four types of experimental specimens are prepared and tested by using an automatic compression machine with 2,000 kN capacity to determine the ultimate load of the built-up slot-in CFS column. The ultimate load is enhanced by increasing the number of self-drilling screws as well as the PF filling. The specimen with 50 mm end spacing, 150 mm middle spacing, and filling of the middle of the hollow part with PF, showed the largest ultimate load. Lastly, all specimens are reported to have local buckling and can resist distortional buckling.

**Keywords:** built-up section, cold-formed steel, polyurethane foam, buckling failure, composite column

---

### 1. Introduction

Cold-formed steel (CFS) is used in construction activity both as structural and as non-structural components, and sometimes it is known as a thin-walled structure due to its thin surface. CFS is becoming popular in construction because of its advantages such as light weight, corrosion resistance, sustainability, flexibility, durability, and ease of production and installation. Besides, CFS is more economical and cheaper than alternative construction materials such as hot-rolled steel, aluminum, reinforced concrete, composite

structure, or timber, because the production of CFS does not involve high energy consumption, high temperature, high technology machines or equipment, expensive software and skilled or expert workers; and the maintenance costs are comparatively low when introduced as structural or non-structural components. Normally, CFS is formed in open sections and unsymmetrical sections such as lipped channel, unipped channel, sigma, zee, and angle cross-section, which are available in the construction market. No CFS with a hollow section or a built-up CFS section is available in the construction market.

However, CFS either in individual elements or built-up sections is exposed to buckling failure when subjected to compression or flexural load. Buckling failure is normally separated into the four categories local, distortional,

---

\*Corresponding author

Email address: [msyahrul210@uitm.edu.my](mailto:msyahrul210@uitm.edu.my)

global, and lateral buckling, which become serious if the failure cannot be resisted in its early stage, and eventually the overall structure will collapse. Many researchers until now still find the best method or propose a new built-up section in which the section approaches the closed and symmetrical condition either in one direction or in two directions. Rahnavard, Craveiro, Simoes, and Santiago (2023) have mentioned that CFS has a low load-bearing capacity because of its thin surface and vulnerability to local buckling failure, and could suitably be combined with another individual element to increase load-bearing capacity for establishing the built-up CFS section. Normally, the basic built-up CFS section that has been promoted in prior studies is a back-to-back profile and face-to-face profile, with the individual sections joined by using fasteners. Examples of prior studies on built-up back-to-back CFS section are Li, Zhou, Ren, Sang, and Zhang (2021a), Yang, Luo, Wang, Shi, and Li (2024a), and Zhou, Li, Ren, Sang, and Zhang (2021).

The built-up face-to-face CFS section or box-up CFS section is introduced either situated face-to-face or situated in a box-up shape by using two individual sections and jointed by using self-drilling screws, self-tapping screws, rivets, spot welds, or bolts and nuts. Examples of studies proposing built-up face-to-face CFS sections include Guzman, Guzman, Arteta, and Carrillo (2021), and Mohd Sani, Muftah, Mohsan, and Kado (2022) of box-up CFS sections (Dai, Fang, Roy, Raftery, & Lim, 2023a; Li, Zhou, Zhang, Ding, & Zhang, 2021b; Selvaraj & Madhavan, 2022; Teoh, Chua, Pang, & Kong, 2024). There are studies on the built-up box-up shaped CFS section that used more than two individual sections, for instance, Yang, Luo, Wang, Shi, and Li (2024b) utilized two lipped CFS channels and two unlined CFS channel sections joined together with four screws, and utilized two unlined CFS channel sections and two  $\Sigma$ -shaped CFS sections joined together with four screws and eight screws. Meza, Becque, and Hajirasouliha (2020) utilized four unlined CFS channel sections joined with four fasteners, and two lipped CFS channel and two unlined CFS channel sections joined with four fasteners.

Another method to minimize the buckling failure is to produce the built-up CFS section by combining or attaching with other materials to a composite structure. Some researchers have studied the CFS as a structural component, either a column or beam element filled with normal and special concrete, as in Qian, Song, Huang, and Wang (2024) with normal concrete grade 30, Chen, Zhang, and Young (2023) with three different grades 40, 80, and 120, Rahnavard, Razavi, Fanaie, and Craveiro (2023) with lightweight concrete grade 30 and density of  $1850 \text{ kg/m}^3$ , Teoh, Chua, Pang, and Kong (2023a) with lightweight expanded clay aggregate self-compacting concrete and Mohd Sani *et al.* (2022) with washed bottom ash concrete. Teoh *et al.* (2024) have stated that the built-up CFS section filled with concrete is capable of expanding the structural performance and able to decrease the local buckling effect at the empty part of the box-up thin surface. Additionally, the built-up CFS is attached to timber board for reducing buckling failure as in the study of Mohd Sani, Muftah, and Osman (2019) with oriented strand board, Gilbert, Hancock, Bailleres, and Hjaj (2014) with softwood (*Araucaria cunninghamii*) veneers, Ferrigato, Minghini, Salomone, and Tullini (2023) with gypsum board, Ma *et al.* (2024) with laminated bamboo lumber, Gao and Xiao (2017)

with ply-bamboo panels and Ng *et al.* (2023) with plywood and hardwood Balau. Lei *et al.* (2024) have reported the result of the axial compression tests on nine specimens of bamboo scriber CFS composite-shaped columns in L-shape, T-shape, and cross-shape cross-sections, attached together using epoxy resin adhesive and bolts. Chakravarthy, Naganathan, Kalavagunta, and Mustapha (2022) have provided experimental data of axial compression load on the built-up box-shaped CFS column using channel section and strengthened with carbon fibre-reinforced polymer for 300 mm, 500 mm, and 700 mm in height. Carbon fibre-reinforced polymer is one of the methods to strengthen the built-up CFS column which is classified as an effective method of increasing the load-carrying capacity. Palanivelu, Moorthy, Subramani, and Dhayanithi (2021) have reported an experimental assessment of circular and square CFS with glass fibre reinforced polymer strips under an axial compression load, and the glass fibre reinforced polymer strips postponed the local buckling.

Polyurethane foam (PF) is a versatile material and is categorized as one type of polymer material produced by reacting isocyanates and polyols through a chemical process. The cell structure of PF is compressible to a certain extent and resilient enough to provide a cushioning effect. PF can be in a rigid or flexible condition which depends on its composition and formulation, and is used in automotive equipment, furniture, footwear, athletic equipment, and packaging. Another significant sector having the potential to use PF is in construction, which represents a high energy consumption and high greenhouse gas emission; thus, it is important to use effective thermal insulation material (Kowalska *et al.*, 2024). Sagadevan and Rao (2020) have studied the structural performance of sandwich beams and column elements that are filled with PF to improve thermal behavior and reduce the weight of the structure. The result of the study showed that the PF as core material in sandwich components prevents premature failures and enhances the structural performance, and the failure mode of the section is not similar to the traditional section. Gontijo *et al.* (2024) have studied the performance of a PF-filled steel web sandwich panel in full scale, such that is formed by using two unlined CFS channel sections, two unlined CFS zee sections, steel face sheets, rivets, and adhesive subjected to quasi-static flexural load.

In conclusion, the study of built-up CFS sections either using two individual sections, for example, basic sections such as back-to-back and face-to-face profile sections, or more than two individual sections in the same shape or different shapes is still in research stage. The idea behind this production is to ensure the structural component is more stable and safer, has low production costs, and resists buckling failure and other structural integrity issues. The built-up CFS section is filled or attached with other materials and researchers are currently looking for a suitable material to reduce production cost and buckling failure. There are many studies trying to use built-up CFS sections as box-up shapes for further investigation; however, there is no information on built-up CFS sections in slot-in shapes that permanently have three parts of hollow section. The concept of the slot-in is referred to the study of Dai, Roy, Fang, Raftery, and Lim (2023b) and of Dai *et al.* (2024), which proposed using two equal sized stiffened channel sections by using self-tapping screws of the length of 22 mm and a diameter of 6.3 mm.

Normal concrete including special concrete that fills in the built-up CFS section can improve the ultimate load but it creates several limitations and challenges such as its weight, construction complexity increment, and structural incompatibility. Thus, PF is classified as the best solution material to fill in the built-up CFS section for improving the thermal insulation and fire resistance of structural components as referred to in the study by Kowalska *et al.*, 2024 and by Sagadevan and Rao (2020). The main objective of the study is to assess and determine the ultimate load of built-up slot-in CFS columns filled with PF and observe their failure mode.

## 2. Experimental Specimen Preparation and Experimental Setup

The experimental specimen preparation and experimental setup are the two primary components of this section. The specimens used in the experiment are prepared using a CFS channel section, a built-up slot-in CFS section, and a built-up slot-in CFS column filled with PF. The experimental setup for this section is focused on and assessed for the ultimate load of a built-up slot-in CFS column filled with PF.

### 2.1 Experimental specimen preparation

The CFS channel section without flange and web stiffener, and with lipped element is selected, and section dimensions and properties are tabulated in Table 1. The important ratio based on the section dimension is also shown in Table 1. This section dimension ratio is calculated to check that the section is suitable for use as a structural component that is able to minimize the buckling failure in the initial part. The percentage differences between  $I_{xx}$  and  $I_{yy}$ ,  $Z_{xx}$  and  $Z_{yy}$ , and  $R_x$  and  $R_y$  is noted to be 79.25%, 69.52%, and 54.69%, respectively. The section dimension ratios of web to flange and web to thickness were calculated and are noted to be 2.00 and 64.52, respectively.

A brush or wipe cloth is used to clean the CFS channel section until it is clear of any debris, dirt, or contaminants. Two CFS channel sections are cut and situated in slot-in configuration for producing the built-up CFS section. Then, the self-drilling screw is used to strengthen the built-up slot-in CFS section which is located and attached at the flange element of one CFS channel section to the flange element of another CFS channel section, with either one or two screws as shown in Figure 1. The new section dimension

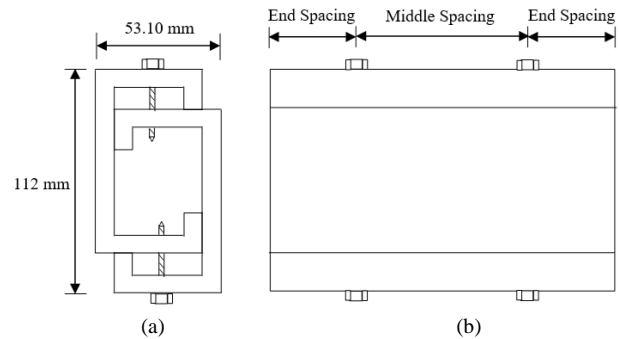


Figure 1. The built-up slot-in CFS section viewed from (a) the top, and (b) the side

of the built-up slot-in CFS section is measured to have 112.00 mm width and 53.10 mm breadth. There are three numbers of hollow parts in the section; top, middle, and bottom. The overall specimen is cut to a fixed 250 mm column height. The PF is bought from the hardware company and filled into a built-up slot-in CFS section at the middle hollow part or overall hollow part as shown in Figure 2, and left at ambient temperature for two days before being tested. The description and symbols of the specimen are tabulated in Table 2.



Figure 2. An example of the built-up slot-in CFS section filled with PF

### 2.2 Experimental setup

The experimental setup is only focused on the assessment of the ultimate load of the built-up slot-in CFS column filled with PF under axial compression load by using the automatic compressive strength machine with a load capacity of 2,000 kN. The end support condition of the experimental setup is pinned-ended support. The pace rate of

Table 1. The section dimensions and section properties of the CFS channel section

Section dimensions and properties			
Parameter	Value and unit	Parameter	Value and unit
Web, $D$	100 mm	Flange, $F$	50 mm
Lipped, $L$	12 mm	Thickness, $t$	1.55 mm
Area, $A$	329 mm <sup>2</sup>	Yield Strength, $f_y$	450 MPa
Moment of Inertia, $I_{xx}$	$0.53 \times 10^6$ mm <sup>4</sup>	Moment of Inertia, $I_{yy}$	$0.11 \times 10^6$ mm <sup>4</sup>
Section Modulus, $Z_{xx}$	$10.63 \times 10^3$ mm <sup>3</sup>	Section Modulus, $Z_{yy}$	$3.24 \times 10^3$ mm <sup>3</sup>
Radius of Gyration, $R_x$	40.21 mm	Radius of Gyration, $R_y$	18.22 mm
Section dimension ratios			
D/F	2.00	D/t	64.52

Table 2. The specimen description, symbols, and self-drilling screw spacing

Specimen description	Specimen symbols	End spacing (mm)	Middle spacing (mm)	Total number of self-drilling screws
Built-up slot-in CFS is attached to the flange element with one number screw at the top and bottom side of the column section and filled with PF at the middle hollow parts only.	BSCFS1	125	0	2
Built-up slot-in CFS is attached to the flange element with two number screws at the top and bottom side of the column section and filled with PF at the middle hollow parts only.	BSCFS2	50	150	4
Built-up slot-in CFS is attached to the flange element with two number screws at the top and bottom side of the column section and filled with PF at the middle hollow parts only.	BSCFS3	100	50	4
Built-up slot-in CFS is attached to the flange element with two number screws at the top and bottom side of the column section and filled with PF at the overall hollow parts.	BSCFS4	100	50	4

the experiment is considered to be 1 kN/s. The selection of the pace rate is based on material behavior consideration, column geometry, and failure mode. Normally, a slow pace rate is for larger and slender columns to allow proper observation of buckling failure and also for homogeneous material or individual sections. The column is placed in the middle part of the steel plate of the automatic compressive strength machine. The result of the ultimate load and failure mode of all specimens especially on web and flange elements is observed and recorded. The comparison study is done by assessing the ultimate loads with built-up slot-in CFS column using the CFS channel section (125 × 53 × 12 × 1.55 mm) without PF attached with one self-drilling screw at the top and the bottom of the column.

### 3. Results and Discussion

The assessment of the ultimate load of built-up slot-in CFS column filled with PF is analyzed and discussed here. The complete set of ultimate loads is in Table 3, with the failure modes of the specimens. The lighter and heavier specimens are BSCFS1 and BSCFS2, respectively, and the percentage difference between the specimens is 3.11%. The mass of the specimen is increased by increasing the number of self-drilling screws by approximately 1.01% when using two of them, and with increasing parts of filling of PF in the specimen by about 2.19% for additional filling at another two hollow parts. The mass of the specimen does not affect the ultimate load.

The highest ultimate load is reached by BSCFS2 and the lowest by BSCFS1. From observation and analysis, the ultimate load of BSCFS1 was the lowest due to the number of self-drilling screws and the end spacing being too large. Additionally, there is no location of the self-drilling screw at the middle part or no middle spacing of the column is reported. The percentage differences between BSCFS1 with BSCFS2, BSCFS3 and BSCFS4 are 9.03%, 1.37% and 2.62%, respectively. The percentage difference between the highest ultimate loads, BSCFS2 with BSCFS3 and BSCFS4 are 7.76% and 6.58%, respectively. BSCFS2 is recorded to have the highest ultimate load because of the lowest value of end spacing due to the increment of the load is generally located at the top and bottom of the column. However, when the PF is filled at the overall hollow parts of the column, the ultimate load of the column is increased by around 1.26%, and

Table 3. The results of the built-up slot-in CFS column filled with PF

Specimen	Mass (kg)	Ultimate load (kN)	Failure mode
BSCFS1	1.371	215.6	Local buckling
BSCFS2	1.385	237.0	Local buckling
BSCFS3	1.384	218.6	Local buckling
BSCFS4	1.415	221.4	Local buckling

indicates that the PF is suitable to fill at three hollow parts including the top, middle, and bottom of the column section. From the experimental results, PF is classified as the best method or solution to increase the ultimate load with lightweight conditions, and has been proven by the study of Mantena, Murty, and Ramana Rao (2022). They have mentioned that the load-carrying capacity of the PF-filled square steel section is improved and local buckling risk is minimized when compared with square steel section without PF. Sagadevan and Rao (2020) have stated that the axial compression capacity of the PF-filled section is twice the value when compared with the empty section and PF-filling also helped to improve the load-carrying capacity with avoiding a premature localized failure of the section. Padmaja, Murty, and Ramana Rao (2021) have reported that the PF-filled tube section possessed a greater load-carrying capacity when compared with PF alone and tube section without PF-filling, and that the load-carrying capacity of the PF-filled tube section increased when the b/t ratio was decreased.

In conclusion, the ultimate load is increased with increasing the number of self-drilling screws, with decreasing the end spacing, and with increasing filling of the hollow parts. When compared with the built-up slot-in CFS column with a bigger size of flange and web element, and one self-drilling screw at the top and at the bottom of the column, the percentage difference is recorded as 14.74% with BSCFS1, 22.45% with BSCFS2, 15.92% with BSCFS3 and 16.98% with BSCFS4. The bigger size of the flange and web element is not affecting the ultimate load of the built-up slot-in CFS column but the number of self-drilling screws, and the location of the self-drilling screw at the end and middle spacing do influence the ultimate load.

The failure mode of all specimens is reported to obtain the local buckling failure because the flange and web element are moved out of the origin line but there is no

movement of the corner of the section especially at the corner of the flange. Normally the failure mode in which the corner of the flange element is moved out either one side or both sides is recognized as distortional buckling failure. This is because the built-up slot-in CFS section is able to solve the distortional buckling failure due to the suitability of the location of the self-drilling screw which is situated at the flange elements in both directions; top and bottom. The failure mode of BSCFS1, BSCFS2, BSCFS3, and BSCFS4 is illustrated in Figure 3. The red circle shows the critical buckling failure of the specimen similar to the study by Qian *et al.* (2024) and Teoh, Chua, Pang, and Kong (2023b). From a comparison with the previous studies, the smallest section of the channel is shown more critical in buckling failure mode when compared with a larger section of the channel. Although the web and flange elements are buckled or bent, there is no failure occurring at the PF part due to its advantages such as its lighter and less brittle nature which makes it very helpful in preventing buckling failure of the entire member. The local buckling occurred at the end of the column specimen for BSCFS1 in which self-drilling screws are placed at mid-span, but for the other specimens the self-drilling screws are not at mid-span and buckling failure happened at mid-span. However, when PF is filled to all hollow parts, the buckling does not occur only at mid-span but also at the end of the column specimen.

#### 4. Conclusions

The analysis and assessment of the ultimate load of built-up slot-in CFS column filled with PF has been reported.

Several conclusions and recommendations are made from the analysis and observation of all specimens as follows.

- (1) The highest ultimate load in this study was 237.0 kN for specimen BSCFS2. The ultimate load increased on increasing the number of self-drilling screws and on increasing filling with the PF. Besides, the ultimate load also depended on the end spacing and middle spacing by the location of self-drilling screws, and from the results of the study, the end spacing should be less than the middle spacing.
- (2) The failure mode of all specimens was recorded to observe that there was local buckling, while specimens without any filling material are normally reported to have local and distortional buckling. The built-up slot-in CFS column which is located and attached to the flange element by using a self-drilling screw is able to resist distortional buckling.

For further study, the height of the column should be added by referring to the slenderness ratio in different categories such as short, intermediate, and slender columns for determining the relevance of ultimate load, and the column should be completed with a linear variable deformation transducer or strain gauge for measuring the deformation. Furthermore, the physical and chemical properties of the PF should be tested and discussed, and comprehensive information should be used for analytical assessment purposes and also mathematical modeling to predict the experimental results. The results of experimental activity in the study should be compared with numerical and analytical analysis.

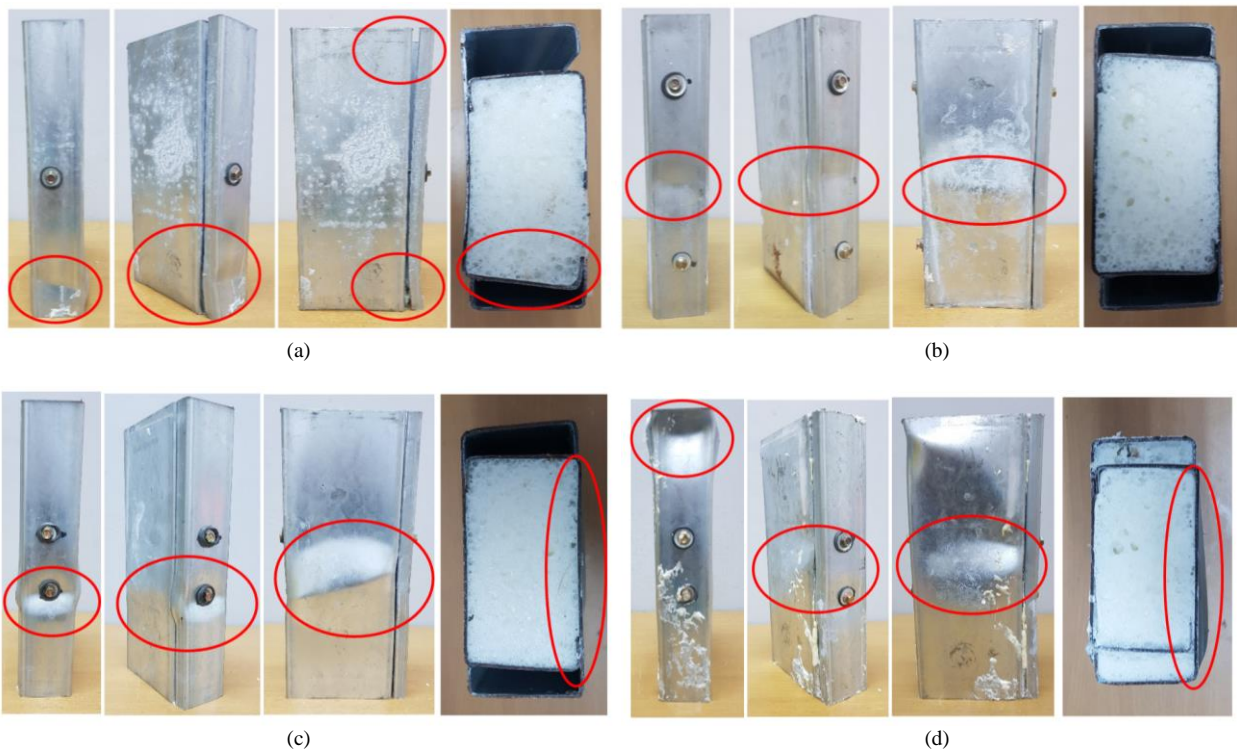


Figure 3. The failure modes of (a) BSCFS1, (b) BSCFS2, (c) BSCFS3, and (d) BSCFS4

## Acknowledgements

The authors kindly thank the Malaysia Ministry of Higher Education under the Fundamental Research Grant Scheme with the sponsorship file number FRGS/1/2021/TKO/UITM/02/101 for the financial support and also Universiti Teknologi MARA (UiTM) Pahang Branch for the facility support. Sincerest gratitude is extended to the Faculty of Civil Engineering, UiTM Pahang Branch members and staff for providing technical advice and assistance.

## References

Chakravarthy, N., Naganathan, S., Kalavagunta, S., & Mustapha, K. N. (2022). Structural performance of experimentally investigated CFRP-strengthened cold-formed steel built-up columns. *Iranian Journal of Science and Technology, Transactions of Civil Engineering*, 46, 917–924.

Chen, M. T., Zhang, T., & Young, B. (2023). Behavior of concrete-filled cold-formed steel built-up section stub columns. *Thin-Walled Structures*, 187, 110692.

Dai, Y., Fang, Z., Roy, K., Raftery, G. M., & Lim, J. B. P. (2023a). Optimal design of cold-formed steel face-to-face built-up columns through deep belief network and genetic algorithm. *Structures*, 56, 104906.

Dai, Y., Roy, K., Fang, Z., Chen, B., Raftery, G. M., & Lim, J. B. P. (2024). Buckling resistance of axially loaded cold-formed steel built-up stiffened box-sections through experimental testing and finite element analysis. *Engineering Structures*, 302, 117379.

Dai, Y., Roy, K., Fang, Z., Raftery, G. M., & Lim, J. B. P. (2023b). Web crippling resistance of cold-formed steel built-up box sections through experimental testing, numerical simulation and deep learning. *Thin-Walled Structures*, 192, 111190.

Ferrigato, D., Minghini, F., Salomone, A., & Tullini, N. (2023). Design tool for gypsum-sheathed cold-formed steel panels under seismic action. *Procedia Structural Integrity*, 44, 386–393.

Gao, W. C., & Xiao, Y. (2017). Seismic behavior of cold-formed steel frame shear walls sheathed with plywood-bamboo panels. *Journal of Constructional Steel Research*, 132, 217–229.

Gilbert, B. P., Hancock, S. B., Bailleres, H., & Hjiaj, M. (2014). Thin-walled timber structures: an investigation. *Construction and Building Materials*, 73, 311–319.

Gontijo, G., Filho, M. A., Benzo, P. G., Pereira, J. M., Machado, J., Denchev, Z. Z., & Sena-Cruz, J. (2024). Development of a foam-filled steel web sandwich panel for the rehabilitation of timber floors. *Journal of Building Engineering*, 86, 108936.

Guzman, A., Guzman, O., Arteta, C., & Carrillo, J. (2021). Experimental study of the influence of welding space in cold-formed built-up box flexural members. *Engineering Structures*, 228, 111541.

Kowalska, B. Z., Szajding, A., Zakrzewska, P., Kuznia, M., Stanik, R., & Gude, M. (2024). Disposal of rigid polyurethane foam with fly ash as a method to obtain sustainable thermal insulation material. *Construction and Building Materials*, 417, 135329.

Lei, C., Wu, Y., Yang, B., Wang, B., Han, J., & Fu, X. (2024). Experimental study on axial compression of bamboo scrimber cold-formed thin-walled steel composite special-shaped columns. *Buildings*, 14, 1–24.

Li, Y., Zhou, T., Ren, L., Sang, L., & Zhang, L. (2021a). Elastic buckling of composite webs in back-to-back cold-formed steel built-up columns—part II: Design formula. *Structures*, 33, 3515–3525.

Li, Y., Zhou, T., Zhang, L., Ding, J., & Zhang, X. (2021b). Distortional buckling behavior of cold-formed steel built-up closed section columns. *Thin-Walled Structures*, 166, 108069.

Ma, R., Wang, X., Du, Y., Sun, G., Kang, S. B., Ma, J., & Chen, Z. (2024). Experimental and theoretical investigation into flexural performance of thin-walled steel-laminated bamboo lumber truss beam. *Thin-Walled Structures*, 199, 111841.

Mantena, P., Murty, V. V. V. S., & Ramana Rao, N. V. (2022). Flexural strength of composite high-density polyurethane foam filled light gauge square steel tubes. *Materials Today: Proceedings*, 51, 2403–2410.

Meza, F. J., Becque, J., & Hajirasouliha, I. (2020). Experimental study of the cross-sectional capacity of cold-formed steel built-up columns. *Thin-Walled Structures*, 155, 106958.

Mohd Sani, M. S. H., Muftah, F., Mohsan, N. M., & Kado, B. (2022). Behavior of built-up cold-formed steel stub columns infilled with washed bottom ash concrete. *Advances in Technology Innovation*, 7(2), 92–104.

Mohd Sani, M. S. H., Muftah, F., & Osman, A. R. (2019). A review and development of cold-formed steel channel columns with oriented strand board sections. *Materials Today: Proceedings*, 17, 1078–1085.

Ng, A. L. Y., Lau, H. H., Fang, Z., Roy, K., Raftery, G. M., & Lim, J. B. P. (2023). Experimental studies of timber to cold-formed steel connections with self-drilling screws. *Structures*, 49, 492–507.

Padmaja, M., Murty, V. V. V. S., & Ramana Rao, N. V. (2021). Quasi static axial compression of empty and PU foam filled circular aluminium and light gauge square steel tubes. *Materials Today: Proceedings*, 43, 2342–2347.

Palanivelu, S., Moorthy, D., Subramani, G., & Dhayanithi, J. R. (2021). Strength enhancement of cold-formed steel tubular column using GFRP strip subjected to axial compression. *Building Materials and Structures*, 64, 251–260.

Qian, Z., Song, Q., Huang, H., & Wang, W. (2024). Axial compressive behavior of spiral stirrup-reinforced concrete-filled cold-formed steel built-up box stub columns. *Engineering Structures*, 308, 118017.

Rahnavard, R., Craveiro, H. D., Simoes, R. A., & Santiago, A. (2023). Concrete-filled cold-formed steel (CF-CFS) built-up columns subjected to elevated temperatures: Test and design. *Thin-Walled Structures*, 188, 110792.

Rahnavard, R., Razavi, M., Fanaie, N., & Craveiro, H. D. (2023). Evaluation of the composite action of cold-formed steel built-up battened columns composed

of two sigma-shaped sections. *Thin-Walled Structures*, 183, 110390.

Sagadevan, R., & Rao, B. N. (2020). Experimental and analytical study on structural performance of polyurethane foam-filled built-up galvanized iron members. *Thin-Walled Structures*, 146, 106446.

Selvaraj, S., & Madhavan, M. (2022). Design of cold-formed steel built-up closed section columns using direct strength method. *Thin-Walled Structures*, 171, 108746.

Teoh, K. B., Chua, Y. S., Pang, S. D., & Kong, S. Y. (2024). Numerical investigation and design of lightweight aggregate concrete-filled cold-formed built-up box section (CFBBS) stub columns under axial compression. *Engineering Structures*, 303, 117509.

Teoh, K. B., Chua, Y. S., Pang, S. D., & Kong, S. Y. (2023a). Experimental investigation of flexural buckling behaviour of self-compacting lightweight concrete-filled cold-formed built-up box section (CFBBS) columns. *Thin-Walled Structures*, 187, 110751.

Teoh, K. B., Chua, Y. S., Pang, S. D., & Kong, S. Y. (2023b). Experimental investigation of lightweight aggregate concrete-filled cold-formed built-up box section (CFBBS) stub columns under axial compression. *Engineering Structures*, 279, 115630.

Yang, J., Luo, K., Wang, W., Shi, Y., & Li, H. (2024a). Research on the flexural buckling behavior of the cold-formed steel back-to-back built-up columns with  $\Sigma$ -section. *Engineering Structures*, 302, 117404.

Yang, J., Luo, K., Wang, W., Shi, Y., & Li, H. (2024b). Axial compressive behavior of cold-formed steel built-up box-shape columns with longitudinal stiffeners. *Journal of Constructional Steel Research*, 212, 108274.

Zhou, T., Li, Y., Ren, L., Sang, L., & Zhang, L. (2021). Research on the elastic buckling of composite webs in cold-formed steel back-to-back built-up columns – part I: Experimental and numerical investigation. *Structures*, 30, 115–133.